

# Photon-Photon and Electron-Photon Physics or Physics at Photon Collider

Maria Krawczyk

*Institute of Theoretical Physics, Warsaw U.*

**Abstract.** A (updated) summary of the Photon-Photon and Electron-Photon physics session is presented.

## INTRODUCTION

The energetic, highly polarized photons can be produced at a high rate in the Compton process as a result of the backscattering of bright laser-photons on high-energy electrons. This is a basic concept of the Photon Collider (Compton Collider) - called also a Photon Linear Collider (PLC) [1, 2]. Such collider is considered as an option to be realized in the  $\gamma\gamma$  and  $e\gamma$  modes at all discussed future  $e^+e^-$  Liner Colliders (LC): TESLA, NLC, JLC and CLIC [3].

The potential of Photon Collider is very rich, in some cases even spectacular [1, 2, 4, 5, 6, 8, 9, 10, 11]. First of all, PLC seems to be the most suitable place to observe a scalar (Higgs) sector. Especially useful should be a  $\gamma\gamma$  mode, where the  $C=+$  resonances, like Higgs boson(s), can be produced, and determination of their basic properties can be performed with a high accuracy. Such a mode allows for a precision measurement of the fundamental effective (loop-) coupling  $\gamma\gamma h$ , which involves contributions from all fundamental, massive charged particles, with masses originating from the Higgs mechanism. In general, such contributions do not decouple and therefore this effective coupling is sensitive to heavy particles, even if their masses are in a range well beyond a reach of the existing and even the next generation experiments. PLC with highly polarized photon-beams offers excellent opportunity for testing of new interactions, including CP-violating one, in the scalar sector. It should discover heavy spin-zero particles, e.g. Higgs bosons from extended models, supersymmetric particles, etc..., in the mass range not accessible at other experiments. This is due to the fact that at PLC such particles can be produced singly, in contrast to a  $e^+e^-$  LC, where they are produced in pairs or with other heavy particles. The  $e\gamma$  mode allows to measure another effective (loop-) coupling, namely  $Z\gamma h$ . This mode is of particular importance for studies of the anomalous  $W$ - interactions in a process  $e\gamma \rightarrow \nu W$ , and for an investigation of the slepton sector. The PLC, both in the  $\gamma\gamma$  and  $e\gamma$  modes, is a perfect place to study QCD, in particular  $t$ -quark interaction and a hadronic “structure” of the real photon.

The realistic simulations of the basic processes for various designs of the Photon Collider are being performed currently, allowing for a reliable comparison with similar simulations done for the main  $e^+e^-$  option and for the hadron colliders.

There are specific aspects of the  $\gamma\gamma$  and  $e\gamma$  colliders, absent at  $e^+e^-$  colliders, which arise mainly from the facts that the photon-beams have a wide spread of energy and a varying with energy degree of polarization. Also, a large hadronic background is expected at a Photon Collider, as photon may (with a probability  $\alpha$ ) behave like a hadron (vector meson dominance idea). To deal with all these issues the dedicated “tools” are needed.

The photon-photon and photon-electron physics working group has a mission to investigate a physics potential of a Photon Collider. There is a large activity in this working group - more than 15 talks were presented during this workshop, most of them in the joint sessions with other working groups like Higgs, SUSY, EW and QCD. A special panel discussion was organized to discuss a need of a Photon Collider.

## PHOTON COLLIDER

The maximum energy of the back-scattered photons produced in the Compton scattering, to be used as a beam for PLC, is equal to  $E_\gamma^{max} = \frac{x}{x+1}E_0$ , where  $x = \frac{4E_0\omega_{laser}}{m_e^2}$ . This energy may reach up to 80 % of the energy of the initial electrons  $E_0$  (for  $E_0 = 250$  GeV and laser energy  $\omega_{laser} = 1.17$  eV ( $\lambda = 1.06 \mu m$ ) and  $x = 4.5$  [1, 2]). For larger  $x$ , the energy spectrum for the photon-beam is more monochromatic, being peaked at a high energy. However, if  $x$  becomes too large (in the above example larger than 4.8) then the  $e^+e^-$  pairs can be created in the collision of the back-scattered photons with the laser photons. This process leads to decrease of the luminosity of the Photon Collider. For  $x = 4.8$  the maximum CMS energy of the  $\gamma\gamma$  collision is equal to 80 % of the energy for the  $e^+e^-$  collision and it reaches 90 % for the  $e\gamma$  case. If lower energy of Photon Collider is needed, one can use the same laser and decrease electron energy keeping all beam parameters as for higher energy (a bypass solution), then the luminosity for  $\gamma\gamma$  collider is proportional to  $E_0$  [2, 7]. One considers also a technique with a tripled laser frequency (NLC/JLC) [7, 12]. This way even at smaller electron beam-energy  $E_0$   $x$  remains large and a resulting energy spectrum for the back-scattered photons is peaked [7, 12].

The Photon Collider can be realized using only  $e^-$  beams. A dedicated interaction point, with a finite crossing angle to avoid background from the disrupted beams, is foreseen at all LC colliders. If electron bunches are tilted with respect to the direction of the beam motion (“crab”-crossing scheme), the luminosity is the same as for the head-on collisions. Luminosities of the  $\gamma\gamma$  and  $e\gamma$  colliders are of the order of 10 % of the  $e^+e^-$  geometric luminosity, which can be larger than the corresponding luminosity for a  $e^+e^-$  collider [7, 2].

The shape (monochromaticity) of the energy-spectrum and the degree of polarization of the back-scattered photons depend crucially on the (product of) polarization of the initial electrons and laser photons. The 80 % polarization for the parent electrons (i.e. twice the electron helicity  $\langle 2\lambda_e \rangle$  equal to  $\pm 0.8$ ) is feasible at LC while a circular polarization of the laser photons,  $P_c$ , can be close to  $\pm 1$ . When  $2\lambda_e P_c = -0.8$  one ob-

tains a highly monochromatic and highly polarized photon-beam. It has a characteristic high-energy peak in the energy spectrum for  $E_\gamma$  larger than  $0.8 E_\gamma^{max}$ , and its circular polarization reaches up to 100 % for the photon energy close to  $E_\gamma^{max}$  (the average polarization is equal to 90-95 % for a high-energy part). Also, a linear polarization of the photon-beams can be obtained by using a linearly polarised laser-light. The maximum degree of a linear polarization of the back-scattered photon,  $\langle l \rangle$ , is obtained at its maximum energy, unfortunately this maximum degree is higher for a lower  $x$  (up to 63.3 % for  $x=1.8$  and only 33.4 % at  $x=4.8$  [2, 7].).

If both photon-beams are obtained from parent particles with  $2\lambda_e P_c = -0.8$ , then the luminosity spectra for the  $\gamma\gamma$  collision has a high-energy peak (for  $z = W_{\gamma\gamma}/2E_0$  larger than  $0.8 z_{max}$ ), with a width at half maximum of about 15 % and the integrated luminosity about 1/3 of the luminosity for  $e^+e^-$  collider [2, 4], e.g. for TESLA  $84 \text{ fb}^{-1}/\text{yr}$ . In the considered case both photon-beams have a high degree of circular polarization,  $\langle \lambda \rangle, \langle \lambda' \rangle \approx -P_c$ , with  $P_c = 1$ , hence  $\langle \lambda \lambda' \rangle$  is close to 1. This means a domination of a state with a projection of the total angular momentum on the  $z$ -axis,  $J_z = \lambda - \lambda'$ , equal to 0.

By flipping the helicities and polarization of the parent electrons and laser photons for one or both photon-beams, one can easily optimize the Photon Collider to work either as a factory or a discovery machine. In particular, to produce in a  $\gamma\gamma$  mode a particle with a definite mass  $m$ , one rather chooses a factory design, i.e. with the monochromatic spectra ( $2\lambda_e P_c = -0.8$ , possibly large  $x$ ), to tune a maximum of  $W_{\gamma\gamma}$  to the mass  $m$  (however first an energy of the  $ee$  collision has to be adjusted:  $\sqrt{s_{ee}} \approx m/0.8$ ). A high rate for the spin-zero state is an extra benefit of this option. On other hand, a maximum degree of linear polarization of the photon-beam, transferred from a linearly polarised laser-photons, is high enough to select in an effective way states with a definite CP-quantum number, i.e. CP-even or CP-odd states, depending whether the polarization-vectors of colliding photons are parallel or perpendicular. To discover new particles, a discovery design of PLC with the broad energy spectra of photon-beams (e.g. with  $2\lambda_e P_c = +0.8$ ) will be more useful.

## TOOLS

The realistic spectra for the photon-beam, which include the higher order QED processes, differ significantly from an ideal (the lowest-order) Compton form. The programmes generating the realistic luminosity spectra for the  $\gamma\gamma$  and  $e\gamma$  colliders exist for all machines (CAIN and PHOCOL with CIRCE and an analytic CompAZ parametrization [13]). The luminosity spectra for the TESLA (both an ideal Compton and a realistic (Telnov) spectrum) and for NLC, are presented in Fig. 1(Left) and Fig. 1(Middle). They correspond to the product of helicities of the initial particles for each photon-beam equal to  $2\lambda_e P_c = -0.8$ . The energy of  $e^-e^-$  is tuned to give a high-energy peak for the invariant mass  $W_{\gamma\gamma}$  equal to 120 GeV (equal to e.g. a Higgs boson mass). The individual contributions, for  $J_z$  equal to 0 and  $\pm 2$ , are shown. Also the average product of helicities of the back-scattered photons  $\langle \lambda \lambda' \rangle$  for a NLC  $\gamma\gamma$  collider is shown in the Fig. 1 (Right).

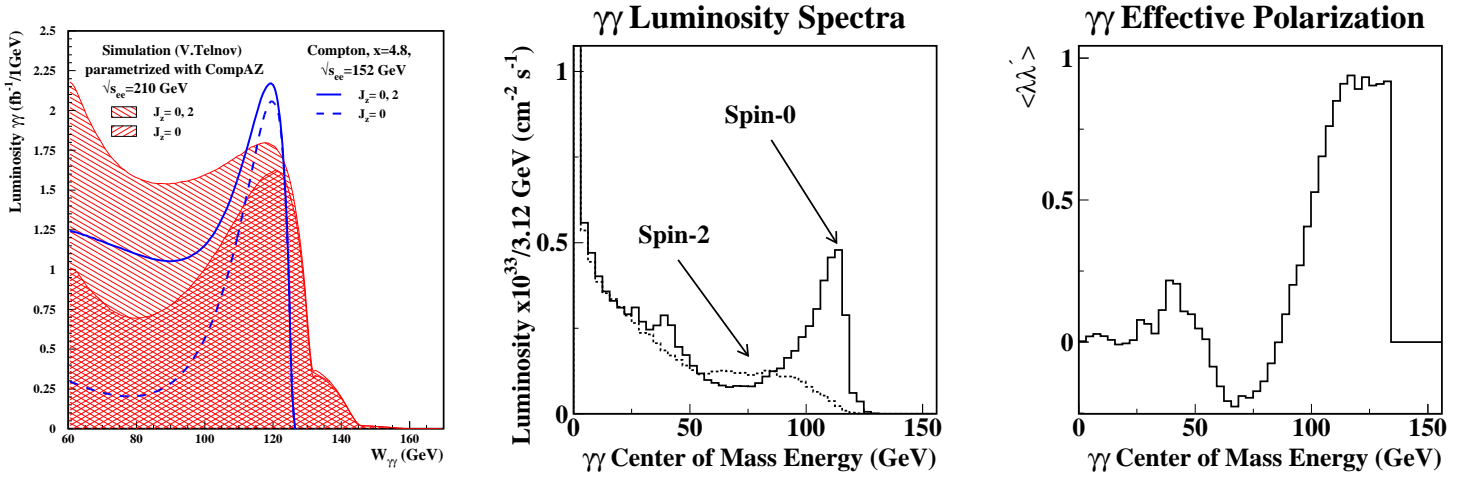


**FIGURE 1.** The peaked spectra considered for a production of a Higgs boson with mass 120 GeV for  $2\lambda_e P_c = -0.8$ . Left: The realistic ( $\sqrt{s_{ee}} = 210 \text{ GeV}$ ,  $x = 1.89$ ) and ideal Compton ( $\sqrt{s_{ee}} = 152 \text{ GeV}$ ,  $x = 4.8$ ) luminosity spectrum for TESLA, for  $J_z = 0, \pm 2$  [22]; Middle: The luminosity spectra for NLC ( $\sqrt{s_{ee}} = 150 \text{ GeV}$ ,  $x = 4.1$ ) for  $J_z = 0, \pm 2$ ; Right: The average polarization  $\langle \lambda \lambda' \rangle$  for NLC, parameters as in (Middle), from [11].

Existing generators like PYTHIA, and GRACE, PANDORA, CompHep [14] are being used by various groups to simulate events in the  $\gamma\gamma$  and  $e\gamma$  collisions; proper matching of the matrix elements for basic hard processes and fragmentation/hadronization processes, as planned e.g. in the program APACIC++[15], is needed.

For a realistic simulation of the photon-initiated processes at PLC, we need to model properly the hadronic interaction of photons. Recently, a new parton parametrization for the real photon was constructed [16]. It uses a full set of available data for  $F_2^\gamma$  and is based on ACOT $_\chi$  scheme. Such scheme, implemented for a first time for a photon, offers an improved treatment of the heavy-quark contributions. A proper description of heavy-quark production in a resolved-photon processes at PLC is necessary to make a reliable estimation of the signal and background in a Higgs-boson search. Of a great importance is also a detailed study of the total cross-section for  $\gamma\gamma \rightarrow \text{hadrons}$ , presented during this workshop [17].

## GOLDEN PROCESSES

There are significant differences between the basic processes which may appear in  $e^+e^-$  and in  $\gamma\gamma$  collisions [8, 9]. At a fixed energy of the corresponding collision, the production rates for a particular state with pair of scalars, fermions or vector particles are larger for the  $\gamma\gamma$  than the  $e^+e^-$  case. In the  $\gamma\gamma$  collision a resonant production of the  $J^{PC} = 0^{++}, 0^{-+}, 2^{++}, \dots$  states may occur [19], in contrast to the  $e^+e^-$  case, with the s-channel resonances  $J^{PC} = 1^{-+}, \dots$ . With a opportunity to produce a zero-spin  $C = +$  resonance, a Photon Collider can be treated as a Higgs factory. In this case, a Higgs boson should be found at other collider, and knowing its mass one can adjust the energy

of the collider using monochromatic spectra, as shown in Figs. 1. It is fortunate, that at the same time, the  $J_z = 0$  state can be produced at a high rate. This enhances a signal while suppresses some of important background processes, e.g.  $\gamma\gamma \rightarrow b\bar{b}$  [9, 21]. Higgs factory gives an opportunity for the precision measurements of the mass, spin, parity, and the CP-nature of the Higgs boson from SM and beyond [4, 9, 10]. A Photon Collider can serve also as a discovery machine for heavier Higgs bosons or other new particles - a broad energy spectrum is preferred then [2, 8, 9, 12]. The advantage of a Photon Collider is that here one can search for a Higgs boson, and study its properties, up to a higher mass than at the  $e^+e^-$  collider, since it can be produced singly at PLC in contrast to main discovery channels at  $e^+e^-$  colliders. In addition, a Photon Collider offers an opportunity to search for a medium mass Higgs boson, with small or zero coupling to ZZ or WW (as H and A in a decoupling scenario of MSSM), which are not accessible at the  $e^+e^-$  LC option, see discussion below.

The fundamental quantity to measure at Photon Collider is the Higgs decay-width  $\Gamma_{\gamma\gamma}$ , and also  $\Gamma_{Z\gamma}$ , which is sensitive to all fundamental, massive charged particles of the underlying theory with masses from the Higgs mechanism [18]. Both decay widths can be measured with a high precision, especially the two-photon width, what allows to distinguish various extensions of the SM, even in their decoupling limits or SM-like scenarios, what we discuss below. If the measurements of these decay widths are combined with results of measurements of the corresponding branching ratios at the  $e^+e^-$  LC, the total decay width for Higgs particle can be derived with accuracy dominated by the expected error of  $\text{Br}(h \rightarrow \gamma\gamma)$ , of the order of 10 % [20, 21, 22, 23].

The W-boson production in the  $\gamma\gamma$  and  $e\gamma$  options of a Photon Collider is sensitive to the anomalous gauge couplings [9, 8, 24]. Photon Collider also allows to perform the dedicated QCD studies, among them on top-quark physics and on the “structure” of a real-photon [25]. Also, a search for new particles, e.g. SUSY particles, are considered as an unique opportunity of the Photon Collider. New interactions, among other the NC QED, models with higher dimensions, and a Higgs-radion mixing (Randall-Sundrum model), etc. can be tested at PLC with a high precision [4, 26, 11].

## SM and SM-like Higgs boson

In light of LEP data a light Higgs (with mass above 115 and below 200 GeV) is expected in the Standard Model. The SM-like scenarios in which one light scalar exists with the basic (tree-level) couplings as predicted in SM, and all other Higgs particles with masses larger than  $\sim 800$  GeV, may be realized in many models with an extended Higgs sector. In particular, in 2HDM or MSSM one can consider a limit of a very large  $M_A$  or  $M_{H^\pm}$ . Yet some deviations, i.e. non-decoupling effects, may appear in the 2HDM, see e.g. [27, 28, 29, 30, 33]. This can show up in the loop-couplings, such as  $\gamma\gamma h$  or  $Z\gamma h$ , due to the additional contributions of the charged Higgs boson, and/or other charged particles from the extended models.

A light SM (or SM-like) Higgs boson with mass below  $\sim 140$  GeV decays dominantly to the  $b\bar{b}$ . With a proper  $b$ -tagging and after correcting for the escaping neutrinos, one can achieve precision of a measurement of the  $\Gamma_{\gamma\gamma} \cdot \text{Br}(H \rightarrow b\bar{b})$  at TESLA at the level 1.6

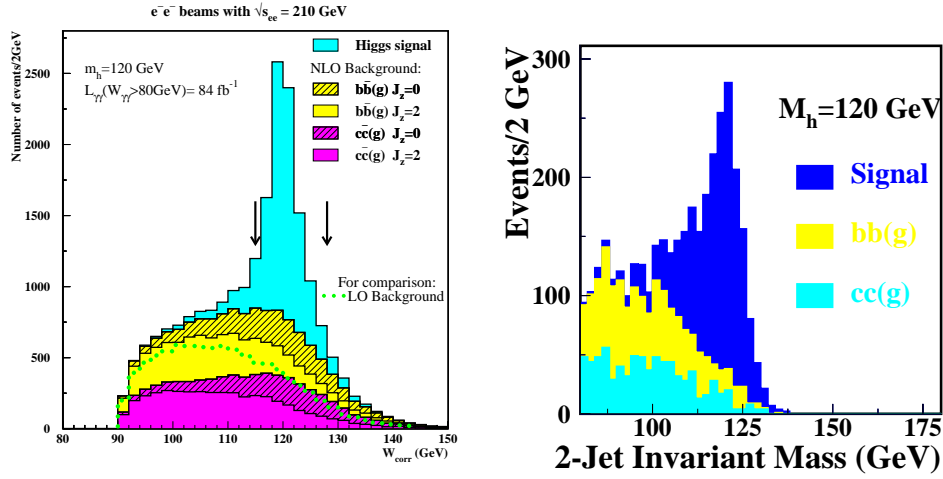


**FIGURE 2.** The SM Higgs resonance at PLC for a peaked spectra (with  $2\lambda_e P_c = -0.8$ ); Left: for TESLA, with NLO background estimation,  $b$ -tagging, and corrections for escaping neutrino ( $\sqrt{s_{ee}} = 210$  GeV,  $x = 1.8$ ), from [22]; Right: for NLC, with LO background ( $\sqrt{s_{ee}} = 160$  GeV,  $x=4.334$ ) [12].

% (Fig.2 (Left)) [22]. For higher Higgs masses the precision for of such measurement worsens, it goes up to 7 % for mass equal to 160 GeV, see Fig.3 (Left) [23].

For heavier Higgs bosons the  $WW$  and  $ZZ$  (also  $W^*$  and  $Z^*$ ) decays channels become important in the SM and SM-like scenarios. The interference between the signal and the (SM-) background, which is very large for the  $WW$  channel, has to be taken into account [31, 32]. The Fig. 3 (Left) shows a comparison of the accuracy of measuring of  $\Gamma_{\gamma\gamma}$  for the  $b\bar{b}$  and  $WW$  plus  $ZZ$  final-states. The yellow line corresponds to the deviation from the SM prediction due to the contribution of a charged Higgs boson  $H^+$ , with mass 800 MeV, expected in the SM-like limit of the 2HDM II [28]. As it shown in Fig. 3 (Right), the measurements of the partial width and of the phase of the amplitude give complementary information and provide a tool with a strong discriminating power between SM and various SM-like scenarios. In the figure the results for the SM-like models with one extra heavy particle with mass 800 GeV ( $H^+$ , quark U or D, lepton L) are shown.

It is clear that the Photon Collider has a large potential in distinguishing the SM-like models, what illustrates Figs.3. As we mentioned above, even in the SM-like limit of the 2HDM II a contribution to  $\gamma\gamma h$  coupling due a heavy  $H^+$  leads to a substantial deviation from the SM prediction, i.e. we observe the non-decoupling effect [28, 29, 30]. The effects arises from  $H^+ H^- h$  vertex, described by term proportional to  $(1 - \mu^2/M_{H^+}^2)$ , where  $\mu$  is a (soft-breaking) mass parameter from the Higgs potential. This non-decoupling effect is larger for small  $\mu$ , and disappears for  $\mu = M_{H^+}$ , see results presented for a ratio of  $\Gamma_{\gamma\gamma}$  in 2HDM and SM in Fig. 4(Left). With an expected precision of the measurement of  $\Gamma_{\gamma\gamma}$ , see e.g. Fig. 3(Left), such decoupling effect can be seen, and moreover one can try to constrain the  $\mu$ -parameter. The radiative corrections to the  $h h h$  vertex in the 2HDM II, with the basic couplings to fermions and gauge bosons W/Z as in the SM, may also lead to a non-decoupling phenomena, as discussed during this

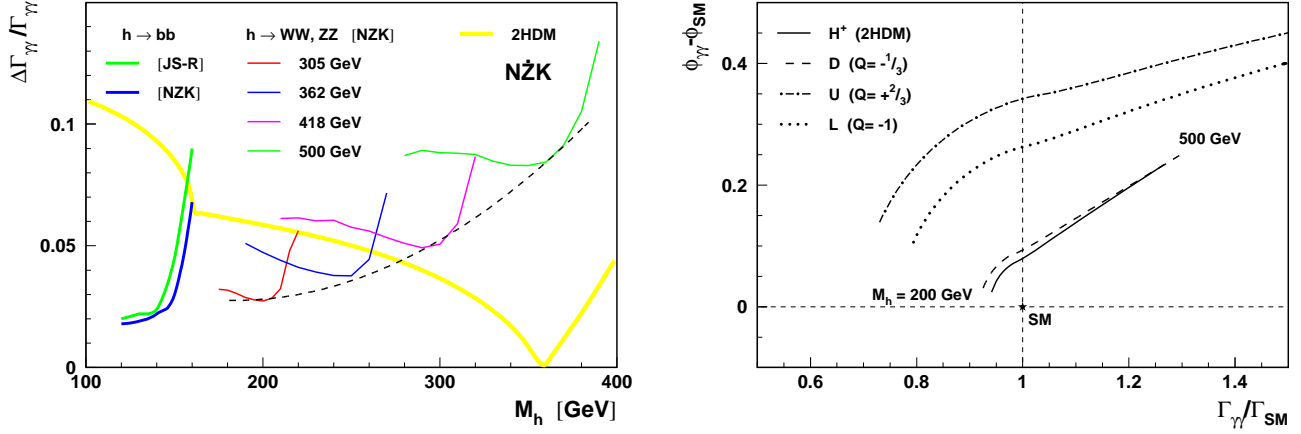


**FIGURE 3.** Left: The accuracy of the measurements of the partial decay width  $\Gamma_{\gamma\gamma}$  as a function of mass of the SM Higgs boson  $h$  (decays into  $b\bar{b}$  [23] and  $WW/ZZ$  [32]). The deviation for a possible SM-like 2HDM II with the charged Higgs boson with mass 800 GeV ( $\mu = 0$ ) is also shown; Right: Deviation from SM of the phase of amplitude and of  $\Gamma_{\gamma\gamma}$ , for various mass of  $h$  and various SM-like models with one extra heavy particle with mass equal to 800 GeV, from [32].

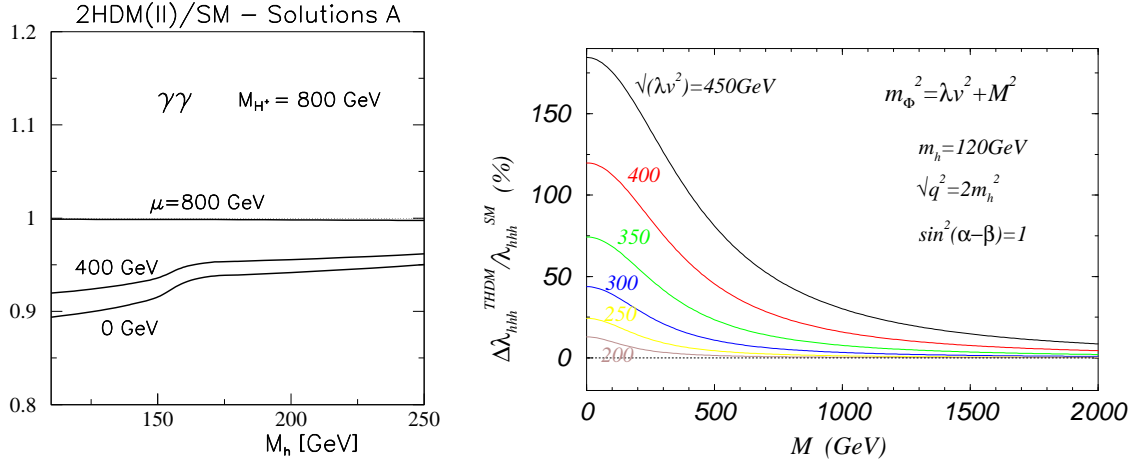


**FIGURE 4.** Left: Deviation from the SM for  $h$  in the  $\Gamma_{\gamma\gamma}$  due to the charged Higgs boson contribution in the SM-like 2HDM II for various  $\mu$ -values [29]; Right: Deviation from the SM prediction of a selfcoupling for Higgs boson with mass 120 GeV as a function of mass parameter  $M$  (equivalent to  $\mu$ ) for various parameters  $\lambda v^2$  [33].

workshop [33]. For a Higgs-boson mass equal to 120 GeV the deviation from the SM prediction for the  $hhh$  vertex can reach even 100 % (Fig. 4(Right)). Note, that in MSSM there is no such effect (decoupling).

The precise measurement of the decay width  $\Gamma_{\gamma\gamma}$  can reveal heavy charged particle circulating in the loop, e.g. supersymmetric particle. There is for example a sensitivity

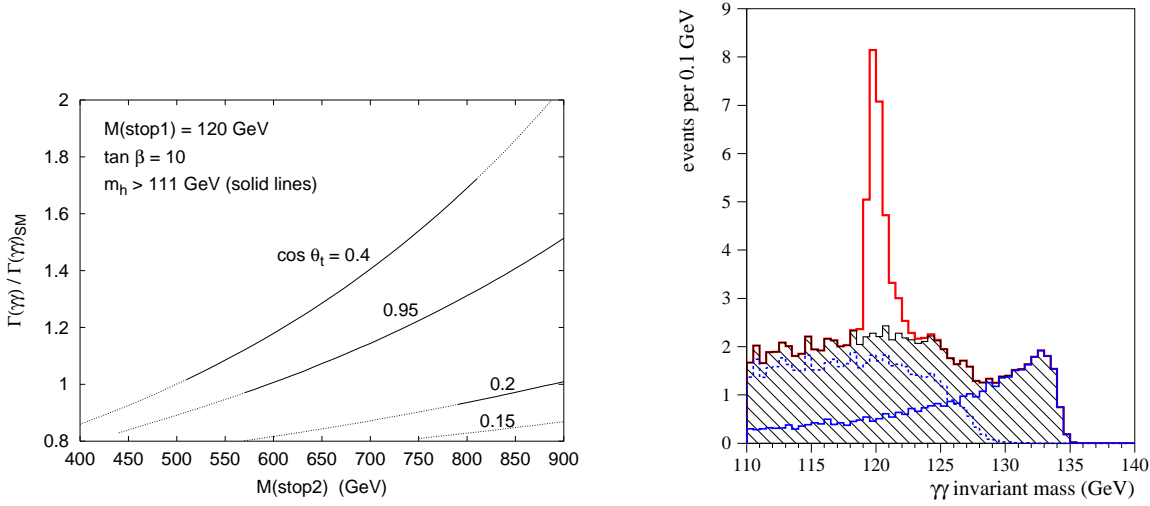


**FIGURE 5.** Left: Deviation from SM of the partial width  $\Gamma_{\gamma\gamma}$  due to the  $\tilde{t}_2$  as a function of its mass, for fixed mass of  $\tilde{t}_1$  equal 120 GeV and for various mixing angle  $\cos \theta_t$  [34]; Right: Number of events of the  $\gamma\gamma \rightarrow \gamma\gamma$  process with a Higgs resonance at mass equal to 120 GeV [37].

to a the heavier stop  $\tilde{t}_2$  contribution, as discussed in [34]. Assuming that the lighter stop  $\tilde{t}_1$  and the mixing angle  $\cos \theta_t$  are already known, the accuracy of the mass determination is estimated to be 10-20 GeV (for 500 GeV LC collider and mass of Higgs boson above 110 GeV). Some of results are presented in Fig. 5 (Left). There are other possible contributions to the  $\gamma\gamma h$  loop coupling, for example the (CP-violating) chargino contribution, see e.g. [35]. The dedicated analysis of such contribution in the decoupling regime of MSSM was performed in [36], and we discuss it below.

The production of the SM Higgs-boson with mass equal to 120 GeV in a process  $\gamma\gamma \rightarrow \gamma\gamma$  being “doubly sensitive to  $\Gamma_{\gamma\gamma}$ ” was analysed in [37]. This analyses leads to an impressive result presented in Fig.5 (Right). The real issue here is a background, as discussed during the workshop.

## MSSM Higgs particles: A and H

The MSSM Higgs-bosons A and H, in the mass range above 200 GeV and with  $\tan \beta$  between 6 and 15, would escape discovery at the LHC (a “LHC wedge”). On the other hand they maybe too heavy to be produced at the first stage of  $e^+e^-$  LC. In this scenario only a light  $h$  is expected to be observed at future colliders with couplings to fermions and W/Z gauge-bosons as in the SM. At the same time heavy Higgs bosons, A and H, will decay predominately into  $b\bar{b}$  final state, and could be discovered at the Photon Collider, as discussed in [38], and [12, 11] (Fig. 6 (Left)). A new simulation for TESLA collider performed in [23] confirms these results, see Fig.6 (Right).

A separating of these two heavy Higgs bosons, A and H, which in the considered scenario are nearly degenerate in mass, maybe be very difficult. According to [38] this can be done by scanning over an energy threshold. Other methods of separation, in which



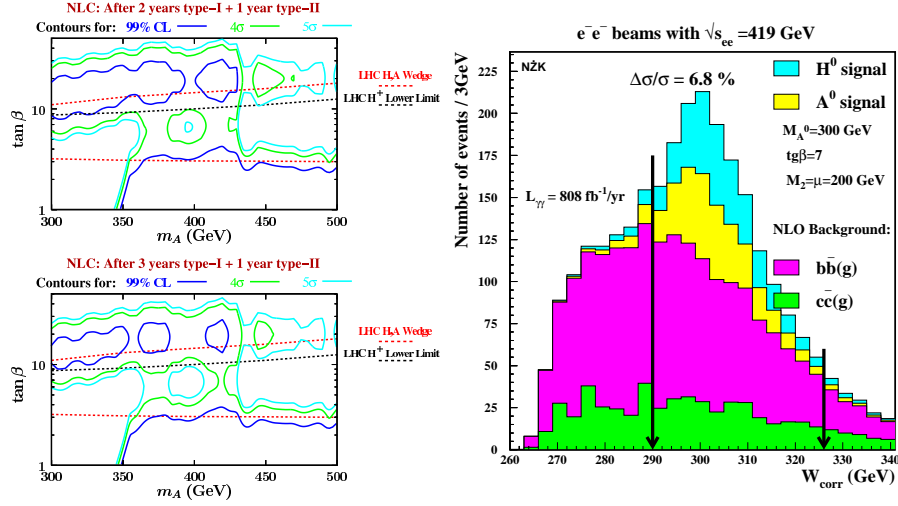


**FIGURE 6.** Production of A and H, with parameters corresponding to the LHC wedge, at the  $\gamma\gamma$  collider. Left: Exclusion and discovery limits obtained for NLC collider for  $\sqrt{ee} = 630$  GeV, after 3 or 4 years of operation (using the broad and peaked spectra) [11]; Right: Simulation of the H and A signals for TESLA collider with energy  $\sqrt{ee} = 419$  GeV (peaked spectrum) for  $M_A = 300$  GeV,  $\tan\beta = 7$  [23].

one uses information on the CP-properties of H and A, are proposed for the heavier Higgs particles decaying into  $t\bar{t}$ , and we discuss them below.

## Charged Higgs boson

The process  $\gamma\gamma \rightarrow H^+H^-$ , within 2HDM II, for the NLC version of the Photon Collider with  $\sqrt{s_{ee}} = 500$  GeV and the product of helicity for electron and laser photon equal to  $2\lambda_e P_c = \pm 0.8$  (the broad (I) and peaked (II) luminosity spectra) were analysed in [39] using the  $\tau^+ \nu_\tau \tau^- \bar{\nu}_\tau$  final state. The background due to  $\gamma\gamma \rightarrow W^+W^-$  was taken into account, with conclusion that a clean, large signal is obtained up to  $M_{H^\pm} \sim 195$  GeV (Fig. 7). This leads to 3-5 % uncertainty in determining of the product of the cross section for  $\gamma\gamma \rightarrow H^+H^-$  and  $[\text{Br}(H^+ \rightarrow \tau^+ \nu_\tau)]^2$ .

## CP properties of Higgs bosons

The  $\gamma\gamma$  colliders with the tunable energy and polarization (circular or linear) of the photon-beams can be especially useful for study of the CP properties of the Higgs sector [40, 10], both to establish the CP quantum-numbers of the neutral Higgs bosons in the case of a CP-conservation, and also to find possible effects due to a CP-violation. Note, that the CP-violating mixing between Higgs particles and a simple overlap in mass for heavy neutral Higgs bosons in a CP-conserving case may lead to similar effects [41]. In testing CP-properties of Higgs particle(s) one can take advantage of polarization asymmetries for a signal [40], use the interference between the amplitude for production

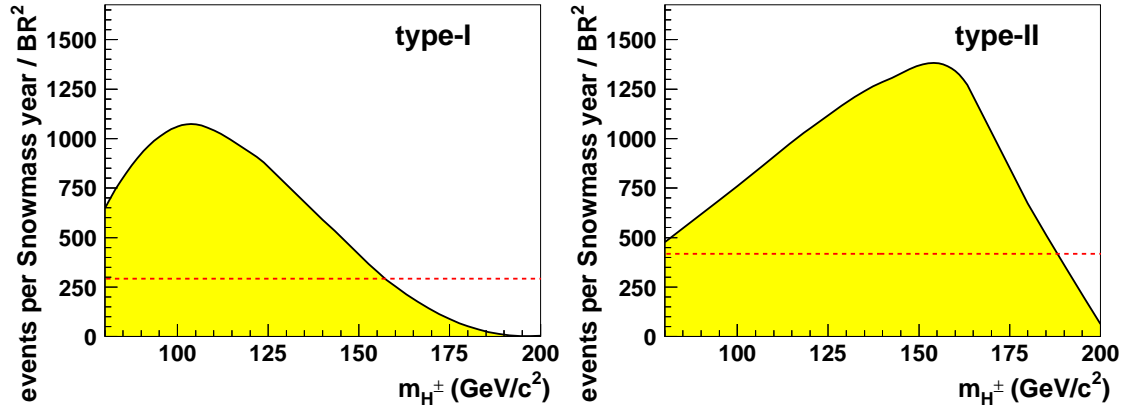


**FIGURE 7.** Number of  $\gamma\gamma \rightarrow H^+H^-$  events obtained for a broad and a peaked luminosity spectra (type-I and -II, respectively) as a function of  $M_{H^+}$  [39].

of Higgs (signal) and of background, and get additional informations from the detailed study of the final-state particles.

If CP is a good symmetry and Higgs bosons have a definite CP-parity, a high degree of a linear polarization of photon beams may be very useful in distinguishing a relatively light CP-even from CP-odd Higgs boson (e.g. H and A in MSSM). This is especially important if such Higgs particles are degenerated in masses, as it happens in the MSSM in the scenario with a light SM-like  $h$  mentioned above, see e.g. Fig. 6(Right). Also, if there are CP-violation effects leading to a mixing between Higgs bosons, linear polarization of the photon beams looks as an ideal tool. Still a circular polarization can be more useful in searching and studying very massive Higgs boson, as a transfer of a linear polarization from a laser-photon to a photon-beam is not efficient for large  $x$ , i.e. for  $\sqrt{s_{\gamma\gamma}}$  larger than half of  $\sqrt{s_{ee}}$ .

To test the CP-property of a Higgs boson one can always use the polarization asymmetries [40]. For heavier masses, one uses additional information from the final-state fermions. For example, identifying Higgs spin and parity in decays to ZZ [42] can be done using the angular distributions of the fermions from the Z-boson decay, which encode the helicities of Z's. Detailed study was performed for above and below ZZ threshold. A realistic simulation based on this analysis, using both the WW and ZZ final-states, was made recently for the TESLA collider in [43].

For heavier Higgs bosons the decay into a  $t\bar{t}$  final-state can be explored. The analysis [44] relies on interference between heavy H and A, with a small mass gap, and between the Higgs resonances and background for a fixed helicities of the decaying  $t$  and  $\bar{t}$ , and it uses a circular polarization of the photon beams. This method of distinguishing Higgs bosons and establishing their CP-properties was found to be efficient for a small  $\tan\beta \sim 3$ , see Fig. 8 (Left). A new analysis [45] is based on interference effects, decay angular distribution of  $t\bar{t}$  and in addition on a phase of the  $\gamma\gamma\phi$  coupling. (The importance of measurement of the phase of  $\gamma\gamma h$  was pointed out in [32] for WW/ZZ channel, see

Fig. 3(Right)). This technique allows to test the CP-properties of heavy Higgs bosons, what was shown in [45] for a particular case of the CP-conserving MSSM.

The CP-violating effects in  $\gamma\gamma \rightarrow \phi \rightarrow t\bar{t}$ , both in the  $\gamma\gamma\phi$  and  $t\bar{t}\phi$  vertices, were studied in [46]. Model-independent analysis of the effects due to Higgs bosons without definite CP-parity was performed using the interference among Higgs particles, as well with a background, for fixed top-quark helicities. Photon beams are assumed to be polarized (both circular and linear polarization is needed) and  $t$  and  $\bar{t}$  helicities are fixed and equal. The extension of a new analysis reported in [45] to the CP-violating case is in under way.

Also in [47] a model-independent analyses was done for the same channel. It was observed that the angular distribution of the decay lepton from  $t/\bar{t}$  is independent of any CP violation in the  $tbW$  vertex and hence directly related to a CP mixing in the Higgs sector. In the analysis the combined asymmetries in the initial state (parent) electron (hence also photon-beam) polarization and the final-state lepton-charge have been applied. If CP-violation is observed, then all the asymmetries, both for circular and linear polarizations, should be used to determine the form factors describing the  $\gamma\gamma\phi$  and  $t\bar{t}\phi$  vertices. This method allows to discriminate models, e.g. SM and MSSM, see Fig. 8(Right), where in a plane of the CP-even and CP-odd observables ( $x_3$  and  $y_3$ ) the blind regions for the SM and the MSSM are shown.

In the CP-violating SUSY, the spin-zero top squarks contribute only to the CP-even part of the  $h\gamma\gamma$  coupling, while charginos can contribute to the CP-odd as well as the CP-even parts [35], leading to a CP-violation. It was demonstrated in [36], that the measurement of the lightest Higgs boson, produced in the collision of the linearly-polarized photon-beams, allows to confirm the existence of the CP-violating chargino contributions to the  $\gamma\gamma h$  coupling even in the decoupling regime of MSSM. Results were obtained in a specific CP-violating scenario, in agreement with existing constraints. The obtained predictions depend strongly on the CP-violating phase  $\Phi_\mu$  both for a ratio of cross section to the SM presented in Figs. 9(Left), and for the polarization asymmetry  $A_2$ , see Figs. 9(Right).

## SUMMARY

The Photon Collider, both in the  $\gamma\gamma$  and  $e\gamma$  modes can provide valuable informations, some of them not accessible at the  $e^+e^-$  colliders, nor at Tevatron or LHC. In light of realistic simulations of various golden processes presented during this workshop and as result of a special panel discussion on a need of a Photon Collider a “little consensus” was reached: a Photon Collider should be planned as an option at each  $e^+e^-$  LC project.

## ACKNOWLEDGMENTS

I would like to thank the Organizing Committee for this excellent meeting and all conveners and speakers for interesting joint sessions. I am especially grateful to Tohru Toka-hashi for a nice collaboration, and also to Jeff Gronberg. Work supported in part by Pol-

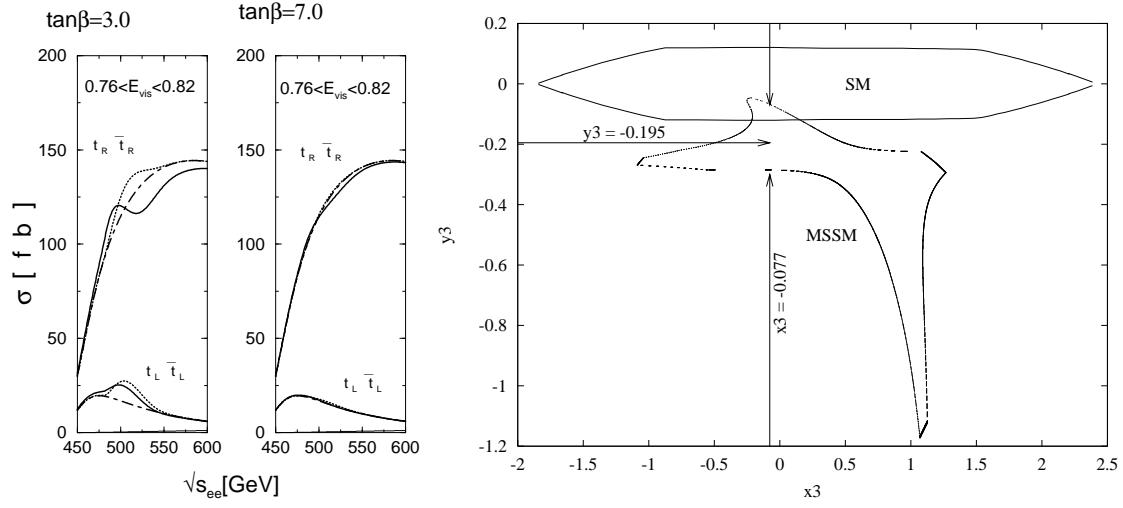


**FIGURE 8.** Left: The inference pattern allowing to distinguish CP-odd from CP-even Higgs particle with mass 400 GeV produced in  $\gamma\gamma \rightarrow t\bar{t}$  [44]; Right: Results from combined analysis of polarization asymmetry and decay lepton charge in a plane of a CP-even and CP-odd observables, showing a bind regions for SM and MSSM [47].

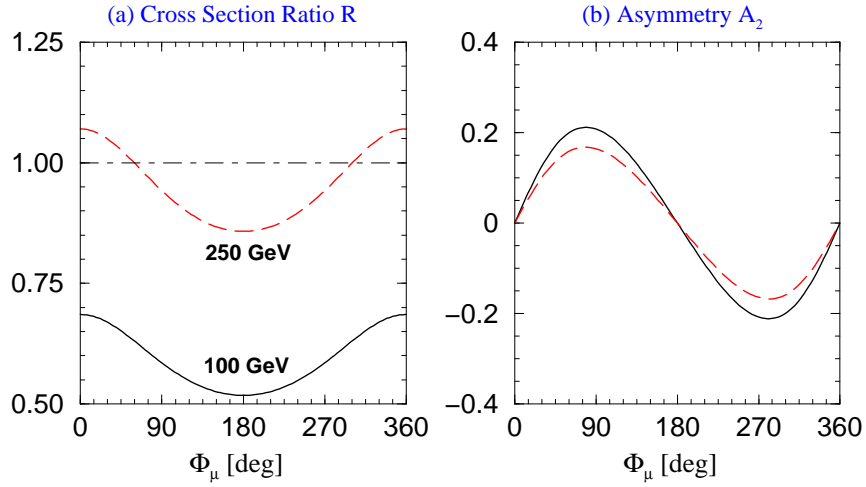


**FIGURE 9.** The dependence on the CP-violating phase  $\Phi_\mu$ . Left: the ratio  $R$  of the cross section  $\hat{\sigma}_0$  to the SM prediction (150 fb); Right: the CP-odd asymmetry  $\mathcal{A}_2$  for  $m_{\tilde{t}_R} = 100$  GeV (solid lines) and  $m_{\tilde{t}_R} = 250$  GeV (dashed lines), respectively [36].

ish Committee for Scientific Research, Grant 2 P 03 B 05119 (2002-2003), 5 P03B 121 20 (2002-2003), and by the European Community's Human Potential Programme under contract HPRN-CT-2000-00149 Physics at Colliders (2002) and EURIDICE (2003).

## REFERENCES

1. I. F. Ginzburg, G. L. Kotkin, V. G. Serbo and V. I. Telnov, *Pizma ZhETF* **34** (1981) 514, (*JETP Lett.* **34** (1982) 491), *Nucl. Instrum. Meth. A* **205** (1983) 47; I. F. Ginzburg, G. L. Kotkin, S. L. Panfil, V. G. Serbo and V. I. Telnov, *Nucl. Instrum. Meth. A* **219** (1984) 5;
2. V. Telnov, *Nucl. Instrum. Meth. A* **294** (1990) 72 and *A* **355** (1995) 3, *A* **472** (2001) 43 (hep-ex/0010033), *A* **494** (2002) 35 [arXiv:hep-ex/0207093].
3. Linear Collider Report from WW Study Group: Understanding “Matter, Energy, Space and Time”
4. Proc. of Int. Workshop on High Energy Photon Colliders, Hamburg, April 2000; *Nucl. Instrum. Meth. A* **472** (2001)
5. B. Badelek *et al.* [ECFA/DESY Photon Collider Working Group Collaboration], arXiv:hep-ex/0108012.
6. S. Kiyoura, S. Kanemura, K. Odagiri, Y. Okada, E. Senaha, S. Yamashita and Y. Yasui, arXiv:hep-ph/0301172; I. Watanabe *et al.*, KEK-REPORT-97-17.
7. T. Takahashi, *Nucl. Instrum. Meth. A* **472** (2001) 4.
8. M. Baillargeon, G. Belanger and F. Boudjema, colliders,” *Phys. Rev. D* **51** (1995) 4712 [arXiv:hep-ph/9409263] and arXiv:hep-ph/9405359.
9. S. J. Brodsky and P. M. Zerwas, *Nucl. Instrum. Meth. A* **355** (1995) 19 [arXiv:hep-ph/9407362].
10. E. Boos *et al.*, *Nucl. Instrum. Meth. A* **472** (2001) 100 [arXiv:hep-ph/0103090].
11. K. Hagiwara, *Nucl. Instrum. Meth. A* **472** (2001) 12 [arXiv:hep-ph/0011360].
12. D. Asner, B. Grzadkowski, J. F. Gunion, H. E. Logan, V. Martin, M. Schmitt and M. M. Velasco, arXiv:hep-ph/0208219.
13. D. M. Asner, J. B. Gronberg and J. F. Gunion, *Phys. Rev. D* **67** (2003) 035009 [arXiv:hep-ph/0110320].
14. **CAIN** P. Chen, G. Horton-Smith, T. Ohgaki, A. W. Weidemann and K. Yokoya, *Nucl. Instrum. Meth. A* **355** (1995) 107; **PHOCOL** V. Telnov, *A code PHOCOL for the simulation of luminosities and backgrounds at photon colliders*; **CIRCE** T. Ohl, *Comput. Phys. Commun.* **101** (1997) 269 [arXiv:hep-ph/9607454]; **COMPAZ** A. F. Zarnecki, *Acta Phys. Polon. B* **34** (2003) 2741 [arXiv:hep-ex/0207021].
15. **HERWIG 6.5**, G. Corcella, I.G. Knowles, G. Marchesini, S. Moretti, K. Odagiri, P. Richardson, M.H. Seymour and B.R. Webber, *JHEP* 0101 (2001) 010 [hep-ph/0011363]; hep-ph/0210213; **PYTHIA** T. Sjöstrand, P. Edén, C. Friberg, L. Lönnblad, G. Miu, S. Mrenna and E. Norrbin, *Computer Phys. Commun.* **135** (2001) 238 (hep-ph/0010017); **PANDORA** <http://www-sldnt.slac.stanford.edu/nld/new/Docs/Generators/PANDORA.htm>; **GRACE** F. Yuasa *et al.*, *Prog. Theor. Phys. Suppl.* **138** (2000) 18 [arXiv:hep-ph/0007053]; **CompHEP** A. Pukhov, E. Boos, M. Dubinin, V. Edneral, V. Ilyin, D. Kovalenko, A. Kryukov, V. Savrin, S. Shichanin, and A. Semenov. Preprint INP MSU 98-41/542, hep-ph/9908288.
16. F. Kraus, talk at LC workshop (St. Malo, 2002).
17. F. Cornet, P. Jankowski, M. Krawczyk and A. Lorca, arXiv:hep-ph/0212160, presented at the workshop.
18. R. M. Godbole, A. De Roeck, A. Grau and G. Pancheri, arXiv:hep-ph/0305071, and this proceedings.
19. A. I. Vainshtein, V. I. Zakharov and M. A. Shifman, *Sov. Phys. Usp.* **23** (1980) 429 [*Usp. Fiz. Nauk* **131** (1980) 537].
20. L. D. Landau, *Doklady Acad. Nauk CCCP*, tom LX, N02, 207, 1948; C. N. Yang, *Phys. Rev.* **77** (1950) 242.
21. T. Ohgaki, T. Takahashi, I. Watanabe and T. Tauchi, *Int. J. Mod. Phys. A* **13** (1998) 2411.
22. T. Ohgaki, T. Takahashi and I. Watanabe, *Phys. Rev. D* **56** (1997) 1723 [arXiv:hep-ph/9703301].
23. G. Jikia and S. Söldner-Rembold, *Nucl. Instrum. Meth. A* **472** (2001) 133, hep-ex/0101056.
24. P. Nieżurawski, A. F. Żarnecki and M. Krawczyk, photon collider at TESLA,” *Acta Phys. Polon. B* **34** (2003) 177 [arXiv:hep-ph/0208234], and this proceedings.
25. P. Nieżurawski, A. F. Żarnecki and M. Krawczyk, LC workshop, April 2003, Amsterdam, “New results for  $\gamma\gamma \rightarrow H \rightarrow b\bar{b}$  in SM and MSSM”.
26. K. Moenig, this proceedings.
27. S. Rindani, plenary talk.
28. S. Godfrey and M. A. Doncheski, *Phys. Rev. D* **65** (2002) 015005 [arXiv:hep-ph/0108268].

27. P. Ciafaloni and D. Espriu, Phys. Rev. D **56** (1997) 1752 [arXiv:hep-ph/9612383];
28. I. F. Ginzburg, M. Krawczyk and P. Osland, arXiv:hep-ph/9909455, arXiv:hep-ph/0101331, Nucl. Instrum. Meth. A **472** (2001) 149 [arXiv:hep-ph/0101229], arXiv:hep-ph/0101208.
29. I. F. Ginzburg, M. Krawczyk and P. Osland, arXiv:hep-ph/0211371, in this proceedings.
30. J. F. Gunion and H. E. Haber, Phys. Rev. D **67** (2003) 075019 [arXiv:hep-ph/0207010].
31. D. A. Morris, T. N. Truong and D. Zappala, Phys. Lett. B **323** (1994) 421 [arXiv:hep-ph/9310244], I. F. Ginzburg and I. P. Ivanov, Phys. Lett. B **408** (1997) 325 [arXiv:hep-ph/9704220].
32. P. Nieżurawski, A. F. Żarnecki and M. Krawczyk, JHEP **0211** (2002) 034 [arXiv:hep-ph/0207294], and this proceedings.
33. S. Kanemura, S. Kiyoura, Y. Okada, E. Senaha and C. P. Yuan, Phys. Lett. B **558** (2003) 157 [arXiv:hep-ph/0211308]. and this proceedings.
34. H. Logan, presented at the workshop.
35. S. Bae, B. Chung and P. Ko, arXiv:hep-ph/0205212.
36. S. Y. Choi, B. c. Chung, P. Ko and J. S. Lee, Phys. Rev. D **66** (2002) 016009 [arXiv:hep-ph/0206025], presented at the workshop.
37. M. Schmitt, presented at the workshop
38. M. M. Muhlleitner, M. Kramer, M. Spira and P. M. Zerwas, Phys. Lett. B **508** (2001) 311 [arXiv:hep-ph/0101083].
39. V. Martin, presented at the workshop.
40. B. Grzadkowski and J. F. Gunion, Phys. Lett. B **294** (1992) 361 [arXiv:hep-ph/9206262], M. Kramer, J. H. Kuhn, M. L. Stong and P. M. Zerwas, Z. Phys. C **64** (1994) 21, W. G. Ma, C. H. Chang, X. Q. Li, Z. H. Yu and L. Han, Commun. Theor. Phys. **26** (1996) 455, Commun. Theor. Phys. **27** (1997) 101, G. J. Gounaris and G. P. Tsirigoti, Phys. Rev. D **56** (1997) 3030 [Erratum-ibid. D **58** (1998) 059901] [arXiv:hep-ph/9703446].
41. A. T. Banin, I. F. Ginzburg and I. P. Ivanov, Phys. Rev. D **59** (1999) 115001 [arXiv:hep-ph/9806515]. I. F. Ginzburg and I. P. Ivanov, Eur. Phys. J. C **22** (2001) 411 [arXiv:hep-ph/0004069].
42. S. Y. Choi, D. J. Miller, M. M. Muhlleitner and P. M. Zerwas, Phys. Lett. B **553** (2003) 61 [arXiv:hep-ph/0210077].
43. P. Nieżurawski, A.F. Żarnecki, M. Krawczyk, LC Workshop, April 2003, Amsterdam, “Measurement of angular distributions for  $\gamma\gamma \rightarrow h \rightarrow ZZ/WW \rightarrow lljj / 4j$ ”.
44. E. Asakawa, J. i. Kamoshita, A. Sugamoto and I. Watanabe, Eur. Phys. J. C **14** (2000) 335 [arXiv:hep-ph/9912373].
45. E. Asakawa and K. Hagiwara, arXiv:hep-ph/0305323.
46. E. Asakawa, S. Y. Choi, K. Hagiwara and J. S. Lee, Phys. Rev. D **62** (2000) 115005 [arXiv:hep-ph/0005313].
47. R. M. Godbole, S. D. Rindani and R. K. Singh, Phys. Rev. D **67** (2003) 095009 [arXiv:hep-ph/0211136], and in this proceedings.